THE IN-PLANE MECHANICAL PROPERTIES OF 2.5D WOVEN POLYMERIC MATRIX COMPOSITES

W. Kong[1, 2], R. Brooks[2], E. Sitnikova[2], X. Zhao[1, 2], Q. Pan[1, 2], T. Yu[1, 2], S. Li[2] and N. Hou[1]

[1]AECC Commercial Aircraft Engine CO.LTD, 3998 South Lianhua RD, Minhang District, Shanghai, 201108, China
Email: kongweiyiacae@163.com

[2]Polymer Composite Research Group, Department of Mechanical, Materials and Manufacturing Engineering, University of Nottingham, University Park, Nottingham, NG7 2RD, United Kingdom

Keywords: 2.5D woven, IM7 Carbon fibre, Mechanical properties

ABSTRACT

With reinforcing fibres in the through thickness direction, 2.5D woven polymeric matrix composites (PMC) are more resistant to penetration and delamination when subjected to impact loadings than laminated composites. However, the mechanical properties of 2.5D woven PMCs, especially those with the carbon fibres which aerospace industries are interested in, e.g. IM7 carbon fibres, are reported rather inadequately. This paper presents the experimental characterisation of four types of 2.5D woven PMCs, namely one with IM7 carbon fibres, one with T300 carbon fibres and two with E-glass fibres. Their in-plane mechanical properties and failure modes under the quasi-static (QS) tensile, compressive and shear loadings are reported.

1. INTRODUCTION

2.5D woven composites are special types of 3D woven composites. Instead of using the third set of yarns (binder), as in conventional 3D woven composites, the reinforcement through the thickness was provided by the interlocking warp yarns. Research [1-2] has shown that 3D woven polymeric matrix composites (PMCs) are more resistant to penetration and delamination than laminated composites. This makes 3D PMCs, especially those made with carbon fibres, promising candidate materials for some key components of aero engines. For example, the fan blade and fan containment casings of the LEAP series [3] developed by CFM International are made from 3D woven carbon fibre PMCs.

Research on the in-plane mechanical properties of 3D woven carbon fibre PMCs has been reported extensively during the 1990s [4-6]. Since then, both carbon fibres and 3D preforming technology have been largely developed. The publications in this period mainly focused on mechanical tests under a specific loading mode such as in-plane tension [7, 8] or in-plane compression [9, 10], rather than comprehensive characterisation. More importantly, as pointed out in very recent publications [11, 12], the available publications on the mechanical characterisation become scarcely representative of the state-of-art in the material, preforming and manufacturing of 3D woven carbon fibre PMCs. The mechanical behaviour of 2.5D woven carbon fibre PMCs are more inadequately reported [13-15].

In this paper, the mechanical characterisation at quasi-static loadings of four types of 2.5D woven PMCs is reported, including one made from IM7 carbon fibres and one made from T300 grade carbon fibres. The test results with respect to the stress-strain behaviour and failure modes under in-plane tension, compression and shear are presented.

2. MATERIALS

For the mechanical tests, flat panels of the 2.5D woven PMCs were manufactured from four types of 2.5D textile preform panels by applying a vacuum-assisted resin transfer moulding (VARTM) process at the University of Nottingham. The preforms were manufactured by SINOMA, China. All of the preforms have the same basic weaving architecture, namely, 2.5D layer-to-layer angle interlock. Two of the preforms are made from 75 Tex E-glass fibres and denoted as GF-1 and GF-2. The other two are made from T300 and IM7 carbon fibres and denoted as CF-T300 and CF-IM7, respectively.

The resin system used was Gurit PRIME^{TM} 20LV epoxy infusion resin with a slow hardener. To ensure uniform thickness in the RTM plates, the moulding tool with dry fabrics inside was compressed by a hydraulic press with 200 kN force. Prior to the injection, the tool was heated to 40°C by a heater in the press. During the injection, the pressure was increased gradually to keep the resin flow speed constant. The injection is finished within 35 minutes from the mixing stage. After the injection, the tool was heated at the rate of 1°C/min up to 100°C and was held at 100°C for two hours to cure the resin. Afterwards, the tool was placed in air to cool to room temperature. The compression was applied to the mould tool throughout the injection, heating and cooling. After cooling, the tool was opened and the cured plate was transferred into an oven to post-cure at 65°C for seven hours. The RTM procedures and the moulding process as described above was followed for every plate to minimise quality variance.

Due to compaction, the geometries of the reinforcements were altered following RTM. The architecture of the RTM-manufactured panels were cut into small samples and then observed by using a Nanotom 160NF X-ray computed tomography (XCT) system. The XCT images for the four composites are given in Figure 1 to Figure 4. It should be noted that Figure 4 is the result of a trial CF-IM7 panel, which has poor manufacturing quality. Voids and defects are widely distributed inside this panel. It is only used here to illustrate the reinforcement architecture. In all the composites, there is a horizontal offset of weft yarns, especially in CF-T300. The views along the warp yarns reveal that the weft yarns are fairly straight except for GF-1, whose weft yarns crimp slightly. At the outermost layers, there are resin rich regions amongst the warp yarns. Whereas, inside the composites, the warp yarns are closely packed.

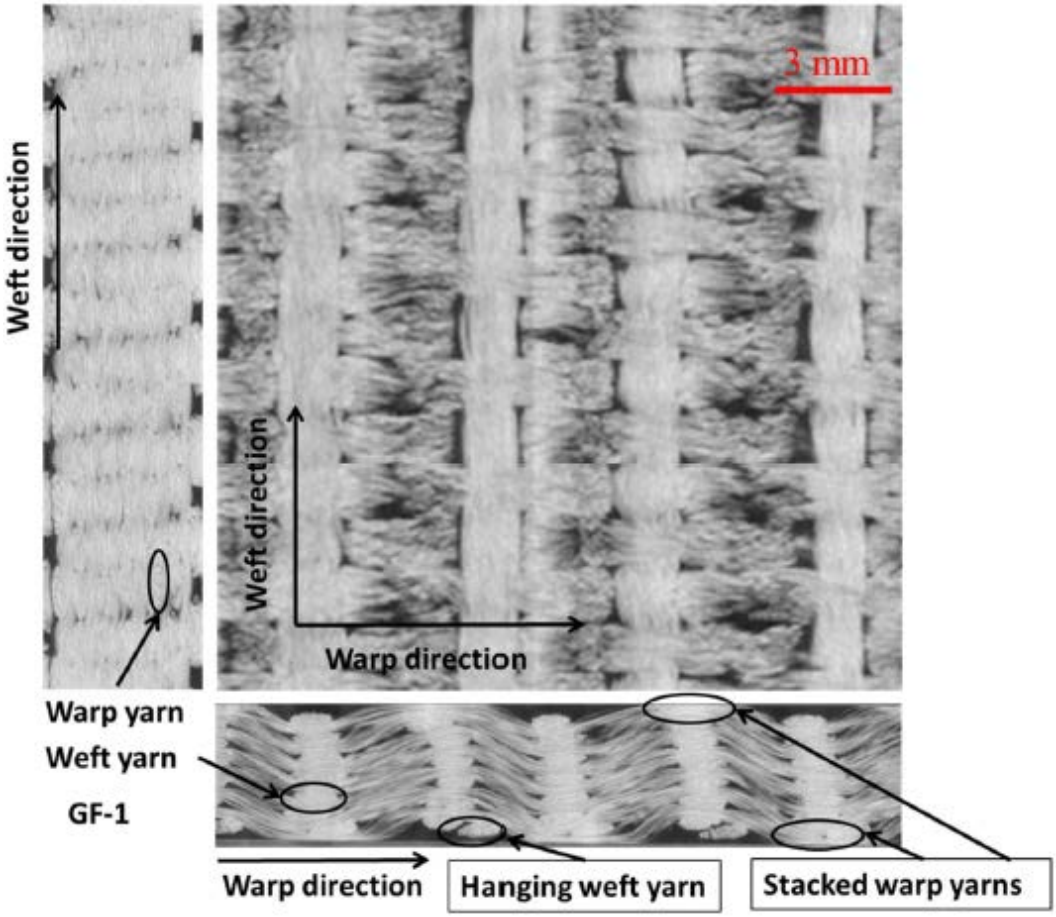

Figure 1: XCT images of GF-1 composites from different views.

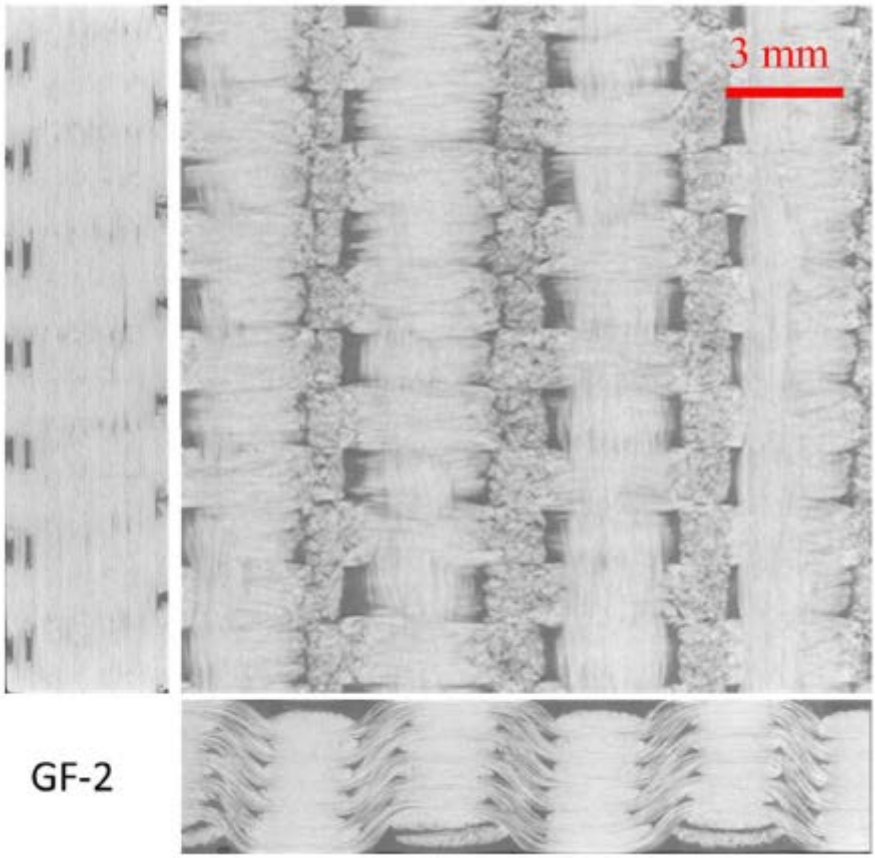

Figure 2: XCT images of GF-2 composites from different views.

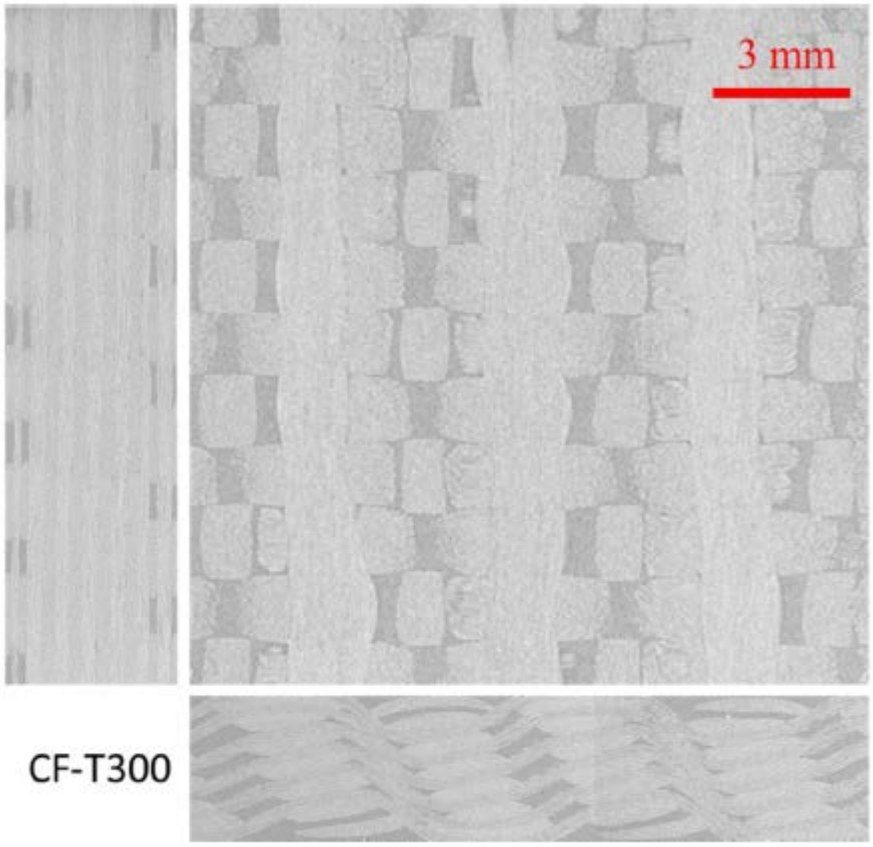

Figure 3: XCT images of CF-T300 composites from different views.

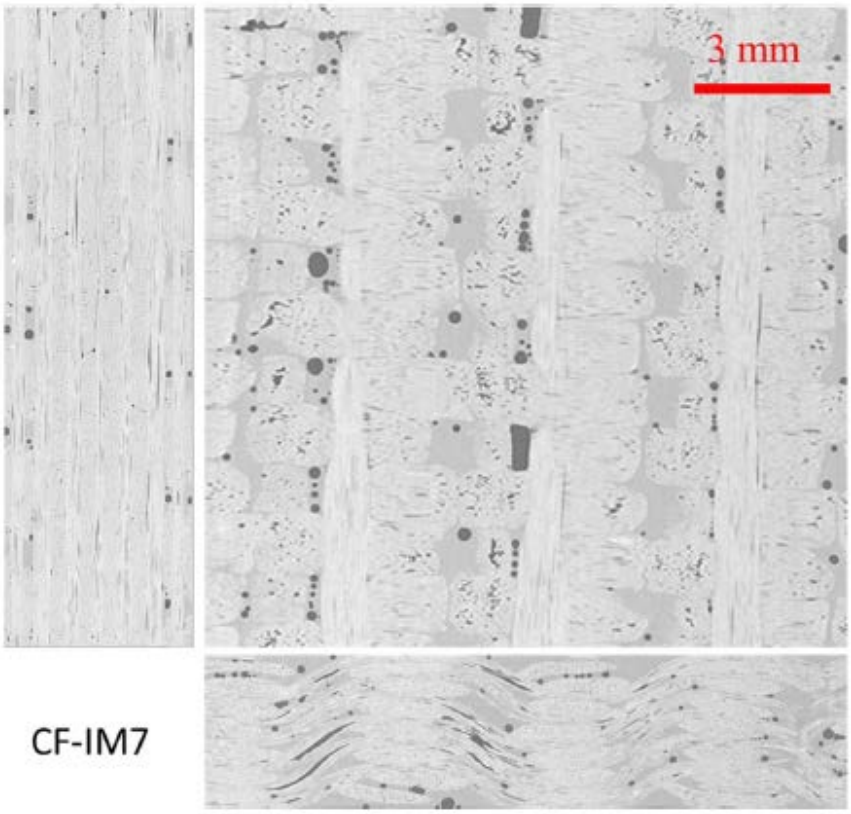

Figure 4: XCT images of CF-IM7 composites from different views.

Measurements were made on the XCT images and then the fibre volume fractions in these composites were estimated. A minimum of 15 cross-sections were measured and averaged. The differences among the four types of composites are summarised in Table 1.

Type	Yarn volume fraction (warp: weft)	Overall fibre volume fraction	Unit cell size (weft × warp) in mm	Moulded panel thickness in mm
GF-1	48.99%:13.24%	50.95%±0.35%	9.04 × 2.62	4.1
GF-2	42.62%:23.39%	54.00%±0.52%	8.7 × 2.62	4.2
CF-T300	38.02%:28.41%	52.21%±0.63%	7.5 × 2.5	3.7
CF-IM7	41.03%:25.64%	55.46%±0.34%	9.04 × 2.56	4.2

Table 1: The volume fractions of yarns and fibres of the four composites, and their unit cell sizes.

3. METHODOLOGY

The four types of composites were tested under quasi-static in-plane tensile, compressive and shear loadings. The tensile testing generally follows the standard ASTM D3039 [21]. The composite specimens were 250 mm-long and 25 mm-wide. Two types of tensile specimens were cut, with weft and warp yarns aligned in the longitudinal direction, respectively.

The compression tests were also conducted in both the weft and the warp directions by employing a jig used in [22, 23]. Rectangular composite specimens of 40 mm in length and 25 mm in width were machined. The load was applied in the longitudinal direction. The specimen was clamped at both ends, leaving a 30 mm-long gauge section. The arrangement of the experimental equipment for this test is shown in Figure 5.

Two types of shear tests were carried out for in-plane shear behaviour. The first one, the ±45° off-axis tensile shear test of ASTM D3518-08 [24], was employed in this study due to its simplicity. The other one is the V-notch rail shear test as described in ASTM D7078/D7078M standard [25]. For the rail shear test, two types of specimens, where either weft yarns or warp yarns were aligned with the loading directions, were manufacture and tested.

In all these tests, force was measured by piezoelectric load cell and was converted to stress. Strain was measured by the video gauge method.

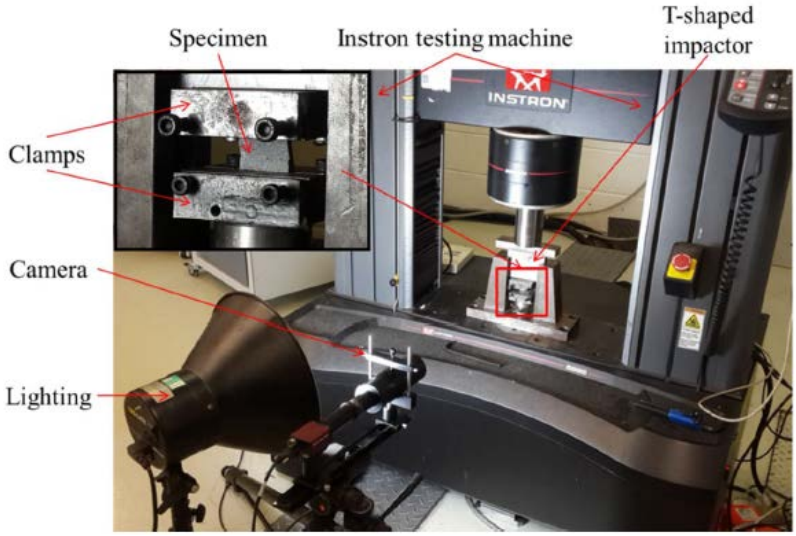

Figure 5: The set-up of the QS compression tests with a close-up view of specimen and the clamp.

4. RESULTS

4.1. Tensile tests

Typical stress-strain curves obtained from the weft and warp tension tests for the four types of composites are plotted in Figure 6 (a) and (b), respectively. Under tension in the weft direction, the stress-strain curves of CF-T300 and CF-IM7 are relatively linear, though some stiffness reduction took place in the later stages of the test. The two carbon composites have higher elastic moduli and ultimate tensile stresses, but lower failure strains than those for GF composites. GF-2 has a higher stiffness and strength in the weft direction than those in GF-1 due to the higher yarn volume fraction of weft yarns in GF-2. In terms of strain energy density to failure, CF-IM7 is higher than the others. This is attributed to the better mechanical properties of IM7 fibres. Non-linearity can be seen in the warp curves for all four composites. Straightening of the crimped warp yarns is observed in the tested specimens of all four composites. This could increase the stiffness. However, as shown in the following, the combination of cracking and straightening results in a reduction in stiffness and the non-linear behaviour.

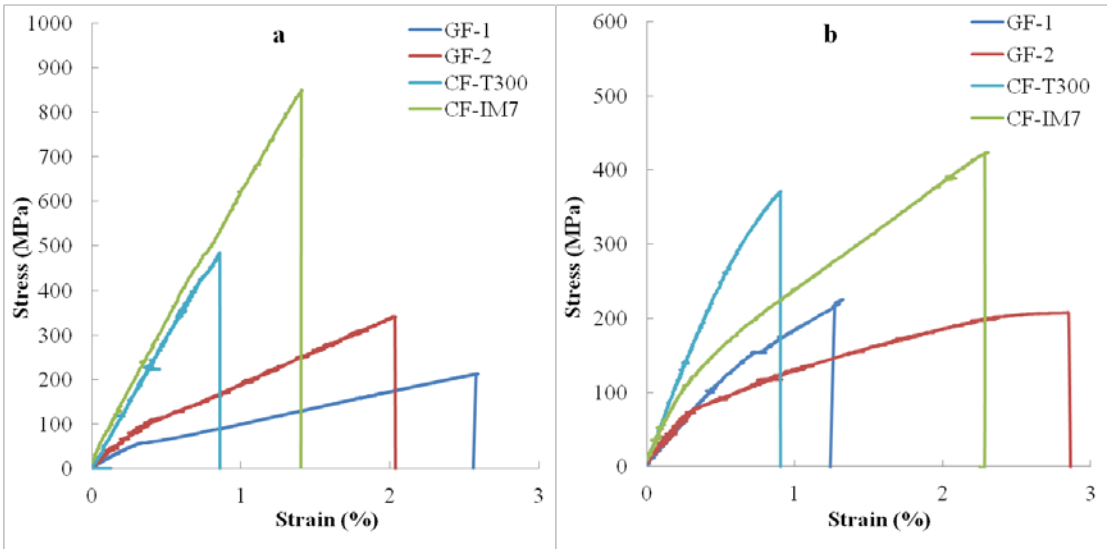

Figure 6: Stress strain curves of the 2.5D woven composites under QS tensile loading in the weft (a) and the warp (b).

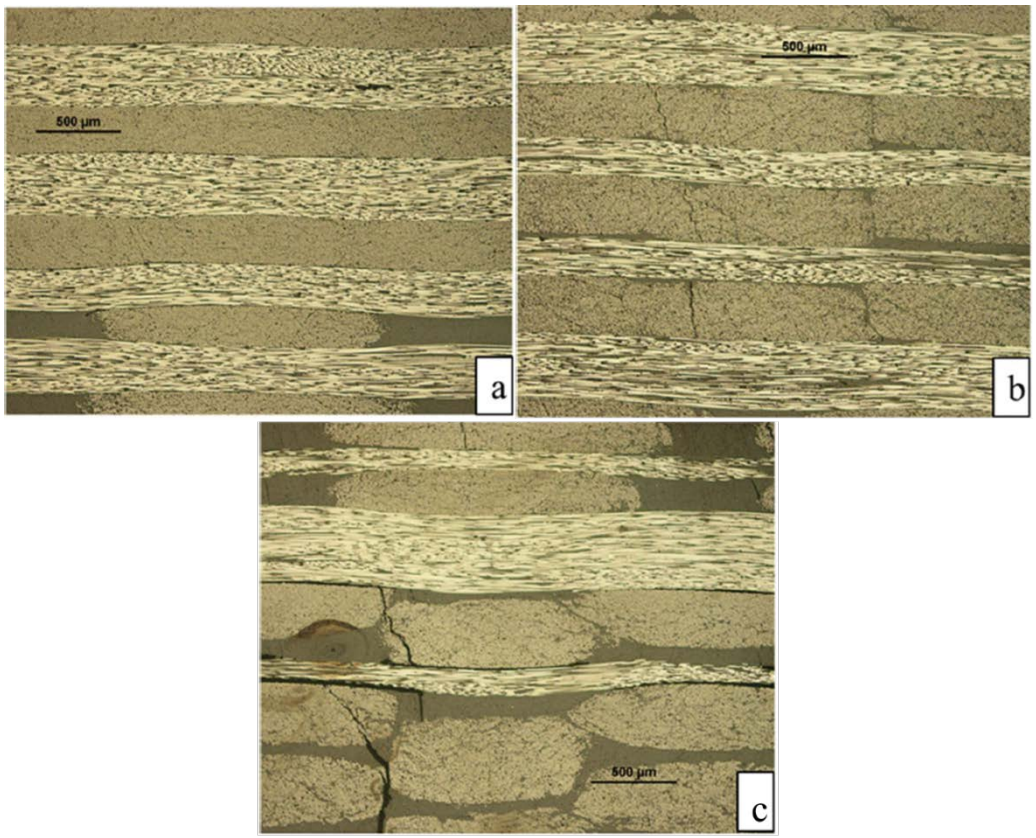

Figure 7: Microscopic observation of CF-IM7 weft tension specimens: (a) loaded to 0.4% of strain; (b) loaded to 0.7% strain; (c) loaded to the final failure.

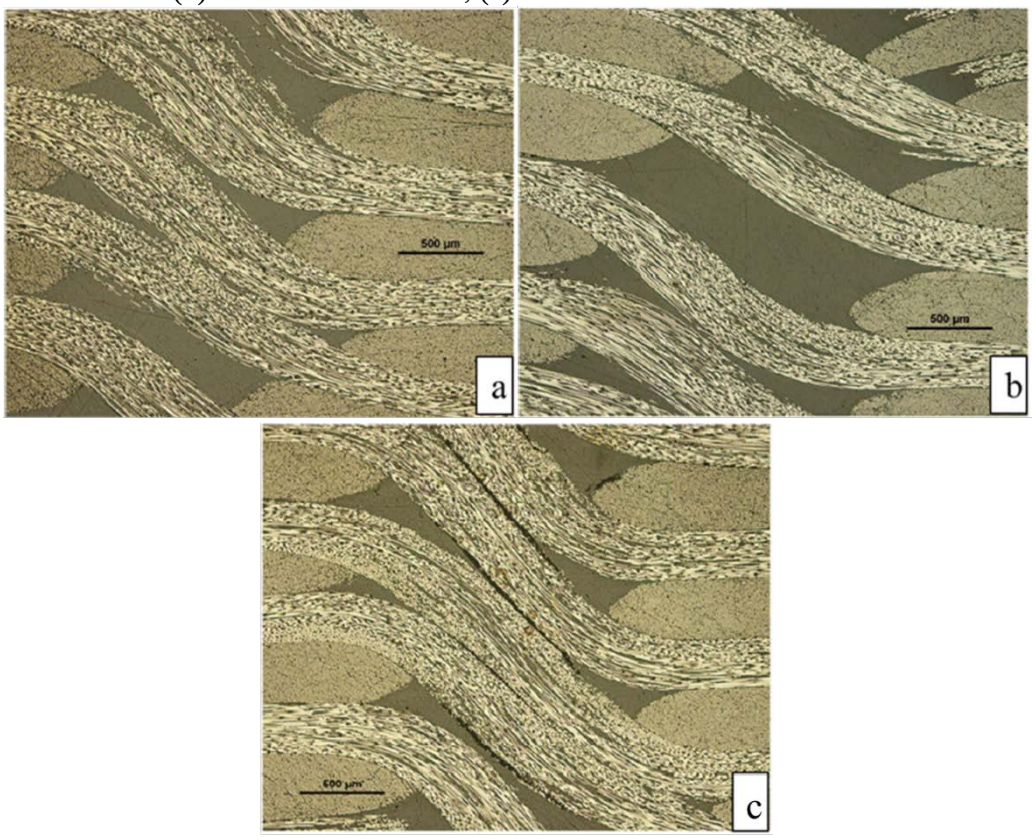

Figure 8: Microscopic observation of CF-IM7 warp tension specimens: (a) loaded to 0.2% of strain; (b) loaded to 0.5% strain; (c) loaded to the final failure

To understand the reason for the non-linear stress strain behavior in Figure 6, some specimens were loaded to a point before the stiffness transition and then unloaded, while some others were loaded to a strain after the transition and then unloaded. These tested specimens were cut along the loading direction and made into samples for microscopic observation. The cutting planes are parallel to both the longitudinal and thickness direction such that the cracks transverse to the loading direction are exposed.

Figure 7 and Figure 8 are the microscopic observations for the tensile specimens of CF-IM7 in the weft and warp respectively. In Figure 7 (a), no crack is found when the specimen is loaded to 0.4% strain, which is slightly before the transition. Figure 7 (b) shows that yarn debonding took place, transverse to the loading direction, propagating along the boundaries of warp yarns. In this case, the specimen was loaded to 0.7% of strain, slightly after the transition. The transverse debonding reduced the effective area which the loading could act on. This is the most likely reason for the transition in the weft stress-strain curves. When the specimen was loaded to final failure, as shown by Figure 7 (c), larger debonding can be observed in more locations. In Figure 6, the transition in warp tension is also likely to be caused by initiation of debonding. At 0.2% of strain, there is no sign of debonding in Figure 8 (a). After transition, at 0.5% strain (Figure 8 (b)), gaps along the path of the crimped warp yarns due to debonding can be seen. When the specimen was further strained to the final failure, more yarn debonding can be observed in Figure 8 (c).

Similar observations are found in the specimens of the other types of 2.5D woven composites. The initiation and propagation of debonding is similar, while there are also extensive transverse intra yarn cracks in the glass composites when the specimens are loaded to failure.

4.2. Compressive tests

The typical stress-strain curves obtained in QS compression experiments for all four composites are plotted in Figure 9 (a) and (b) for weft and warp compressive tests, respectively. In both figures, the curves are generally linear until failure. Similar to the tensile moduli, the moduli of weft compression show correlation with the properties of fibres and the volume fractions of the yarns. The two carbon fibre composites have larger moduli than the two glass composites due to the higher mechanical properties of carbon fibres. The GF-2 modulus is larger than GF-1 because of the higher fraction of weft yarns in GF-2. However, the rest results of the compression tests show little correlation with the fibre properties and yarn volume fraction. Although the fibres of IM7 outperform T300 significantly with respect to mechanical properties, regarding the manufactured composites CF-IM7, their weft strength, the warp strength and the warp modulus are less than those of the composites CF-T300. Meanwhile, there is only small difference among the warp moduli of GF-1, GF-2 and CF-IM7.

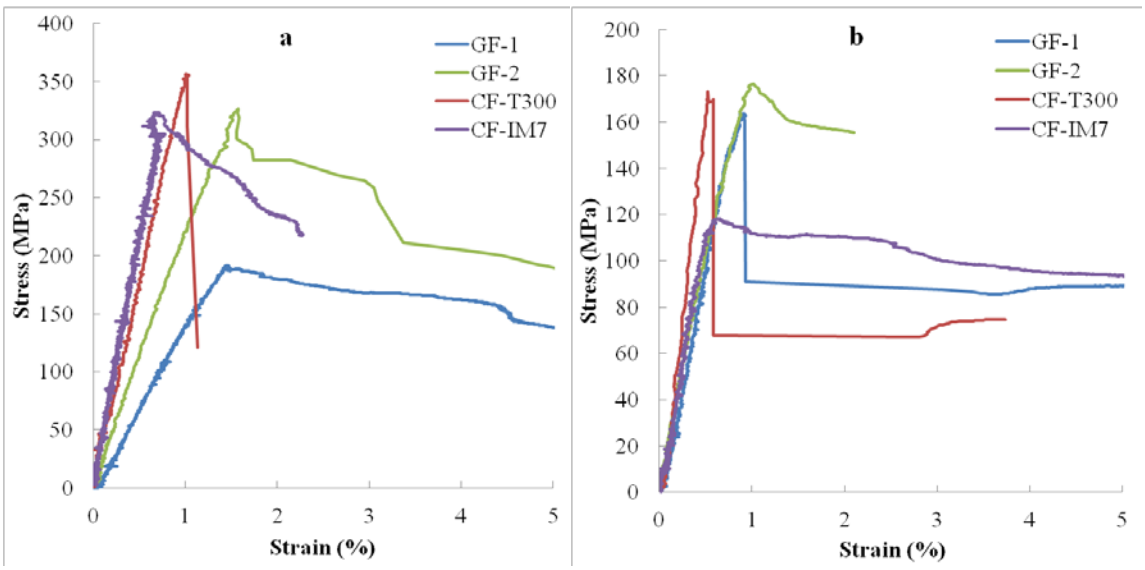

Figure 9: Stress strain curves of the 2.5D woven composites under QS compressive loading in the weft (a) and the warp (b).

After the maximum stress in Figure 9 (a) and (b), load carrying capability remains in all the specimens. As shown in Figure 10, in spite of the failure, some of the fibres are not disconnected. They are able to provide the residual load carrying capability. Under further loading, more damage is caused and the capability degrades, as reflected by the gradual reduction of stress after failure in Figure 9 (a) and (b). Exception of stress drop happened for the warp compression of GF-1 and both compressions of CF-T300. However, the drop is not a sign of brittle failure. It is most likely due to the unloading caused by the failure of maintaining stable stroke control after the specimen buckles.

Regarding failure, similarity can be found in the tested specimens of all four composites. Shear in the through-thickness direction is visible in the photographs of the failed specimens in Figure 10. It is easy to see in the side view of the specimens that the failure surfaces in all the specimens are inclined to the loading direction. The mechanisms of failure in the two directions are, however, different. In the warp specimens, the crimping of yarns can easily lead to their debonding. The debonding of different layers of warp yarns eventually merges, forming a failure surface inclined to the loading direction. On the other hand, fibre kinking is clearly the failure mode in the weft specimens. This is the expected mode when straight yarns or fibres fail under compression.

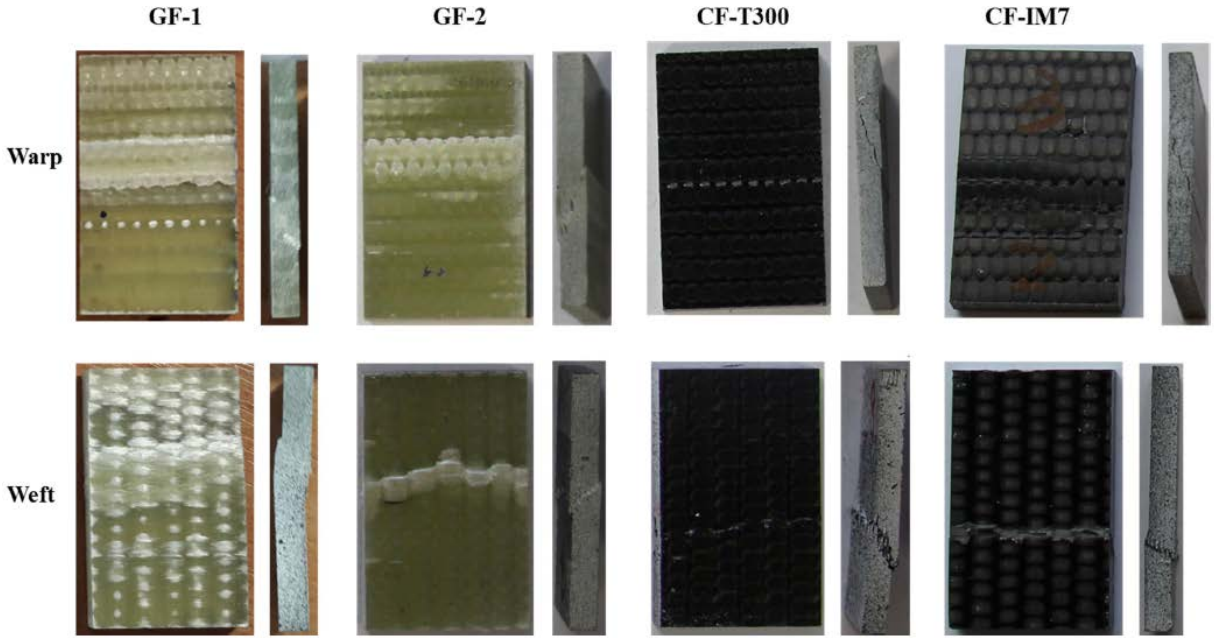

Figure 10: The tested compression specimens.

4.3. Shear tests

The stress-strain curves obtained in the tensile shear and the V-notch shear tests are shown in Figure 11 (a) and (b) respectively. It needs to be pointed out that in many cases the tests were stopped before the final failure of specimens has occurred. As can be seen in Figure 11 (b), V-notch shear tests were stopped 10% of shear strain, above which pure shear state is unlikely. In the tensile shear tests for GF-2 and CF-T300, the strain measurement failed at relatively low values of strain, as shown in Figure 11 (a). The cause for this could be paint cracks, which were generated due to matrix cracks on the surface of the specimens and lead to the failure of optical strain measurement. Nevertheless, the obtained stress-strain curves are sufficient for understanding their shear behaviour. The GF-1 curves are exceptions in both figures, which eventually drop to zero, indicating specimen breaking into two pieces.

In both figures, the curves are generally non-linear except the initial segments. The shear moduli are determined over a strain range from 1500 to 6500 micro strain. Due to the dominance of matrix in the in-plane shear behaviour, the shear moduli determined for all types of the composites were within the range from 3 to 4 GPa (as listed in Table 2). Beyond the elastic range, the curves become non-linear. This is due to the matrix cracking as well as the rotation of yarns, which tend to align with the loading direction. Stress levels increase but tangential stiffness degrades till the end of the tests. At the

end of the tests, the breakage of specimens occurred in three cases, namely, in the off-axis tension of GF-1 and GF-2 composites, as well as in the two-rail shear test of GF-1. The strength values were determined by offsetting a straight line with shear moduli by 0.2% shear strain as recommended by the rail shear test standard ASTM D7078. The strength values of GF-2, CF-T300 and CF-IM7 obtained in the off-axis tension test are very close to those of the two-rail shear test.

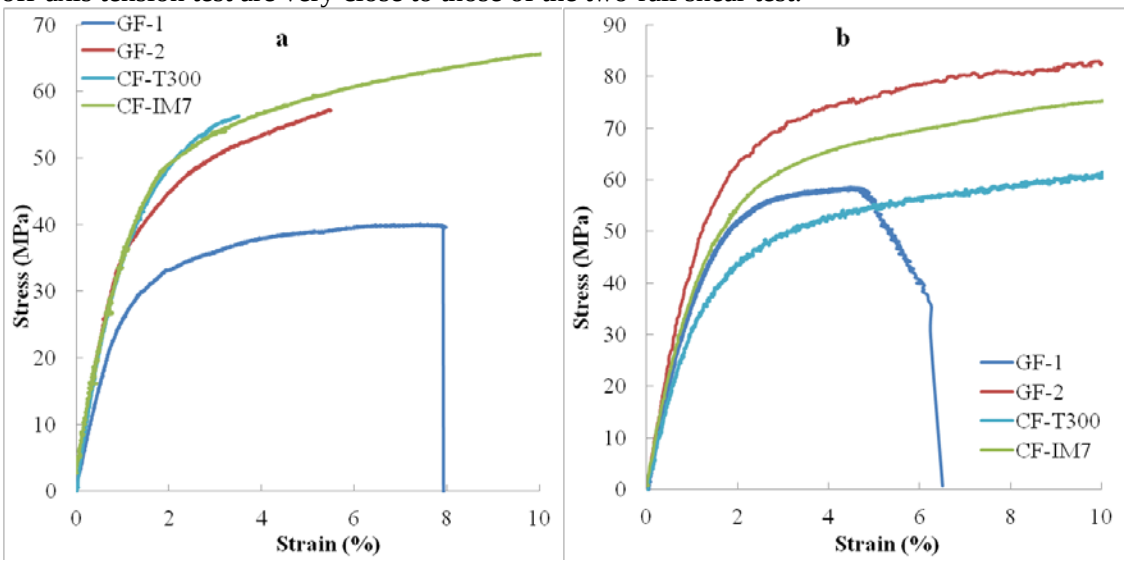

Figure 11: Stress strain curves of the 2.5D woven composites under in-plane shear loading from (a) 45° off-axis tension test and (b) V-notch rail shear test.

Property	Test type	GF-1	GF-2	CF-T300	CF-IM7
Modulus(GPa)	45° tension	2.99±0.98	3.65±0.32	3.7±0.53	3.38±0.22
	Two-rail	4.03±0.14	4.06±0.50	3.41±0.54	3.85±0.42
0.2% Offset strength (MPa)	45° tension	28.57±0.83	38.28±1.64	39.41±0.88	42.81±2.62
	Two-rail	39.6±1.82	37.04±3.6	37.56±5.86	46.6±3.04

Table 2: The in-plane properties from the two shear tests.

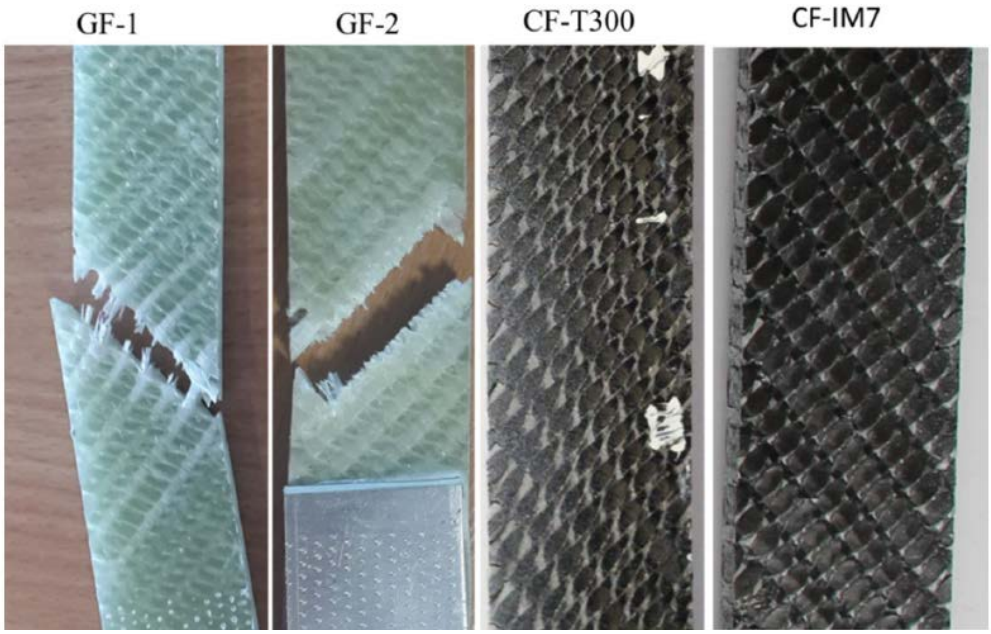

Figure 12: The tested specimens of 45° off-axis tensile tests

The tested specimens of the off-axis tension test are shown in Figure 12. Both GF-1 and GF-2 are broken into two pieces with failure surfaces inclined to the loading direction. During the off-axis

tensile loading, both weft and warp yarns are under tension. The weft direction of GF-1 is relatively weaker hence the failure surface is almost normal to the weft yarns. On the other hand, the warp direction of GF-2 is weaker therefore failure took place normal to the warp yarns. Extensive resin cracking is also observed. Breakage failure does not happen in the CF-T300 and IM7 specimens due to the superior mechanical properties of carbon fibres. Yarn rotation and aligning with the loading direction can be clearly seen in the photographs of the specimens in Figure 12. The resin around the yarns was therefore crushed.

Photos of the tested specimens in the two rail shear test are given in Figure 13. As was mentioned above, two types of specimens were machined for the two-rail shear test, where either the weft or the warp yarns were normal to the loading direction. Five specimens of each type have been tested. The results in Table 2 indicate small standard deviations in the ten specimens, regarding to both the moduli and the strengths. This suggests the irrelevance of yarn direction to this test. In Figure 13, GF-1 broke into two pieces at about 6.3% of strain while the others remain in one piece until more than 10% shear strain. A band of damage between the notches could be seen in each specimen along with kinking of yarns.

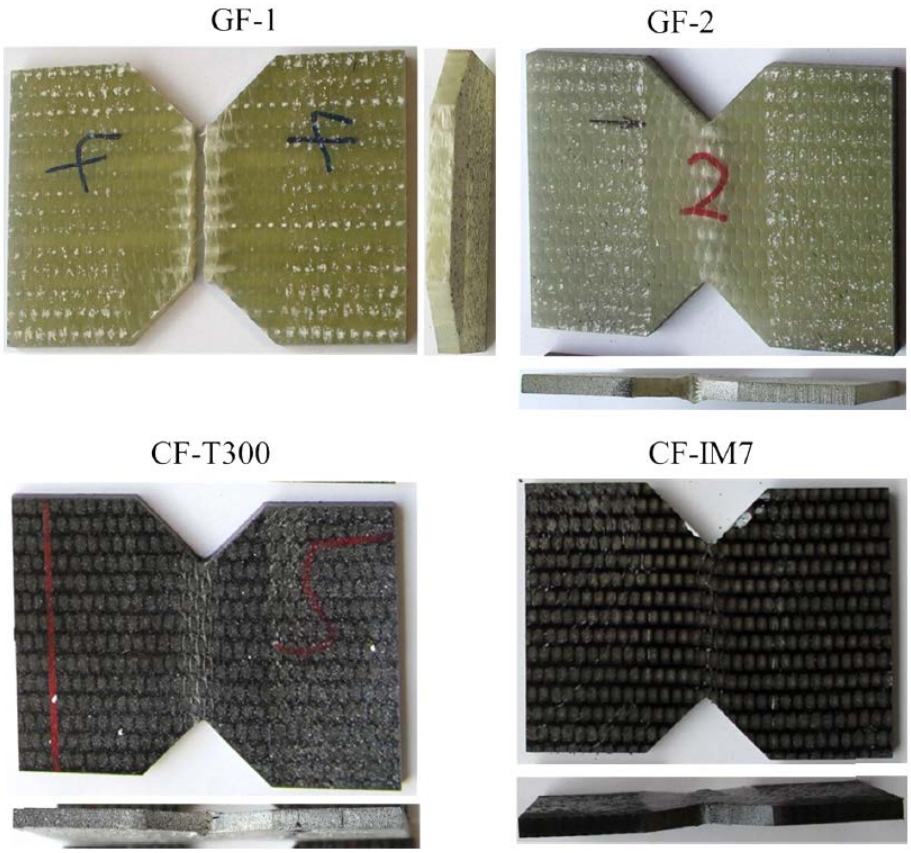

Figure 13: The tested specimens of V-notch two-rail shear tests.

5. CONCLUSIONS

In this paper, the characterisation of four types of 3D woven composites under quasi-static in-plane tensile, compressive and shear loadings is reported. The tension test reveals that the tensile properties in both the weft and warp direction are positively related to the properties of the fibres and the volume fraction of yarns. In terms of strain energy density at tensile failure, CF-IM7 outperforms the others. By microscopic observation on specimens loaded to different levels of strain, it was found that, after the initial linear elastic behaviour, debonding and matrix cracks take place, leading to degradation of stiffness. The compressive properties, however, show little correlation with the fibres and yarn volume fractions, except for the weft compressive strength. The compressive stress-strain curves are generally linear until the maximum strength, where specimens essentially failed as through-thickness shear via

fibre kinking for the weft compression or via connection of debondings for the warp compression. Considerable load carrying capability remains after the failure.

Two methods, namely 45° off-axis tensile shear and two-rail shear were used for testing the in-plane shear behaviour. No major difference was found between the shear moduli measured by these two methods, or between the measured 0.2% offset strength values. All the curves are initially linear but become non-linear later on. Due to the dominance of matrix in the in-plane shear behaviour, there is little difference among the shear moduli of the four types of 2.5D woven composites. Fracture only happened in the glass composites in the directions transverse to the weaker yarns, i.e. the weft of GF-1 and the warp of GF-2. Yarn rotation takes place in the other specimens and makes the tests little representative of a pure shear state at later stages of the tests.

ACKNOWLEDGEMENTS

The authors would like to acknowledge the financial support provided by (1) AECC Commercial Aircraft Engine CO. Ltd through Grant No. RGS106619, (2) International Science & Technology Cooperation Program of China through Project No. 2015DFA71500, and (3) Shanghai Science and Technology Committee through Grant No. 14DJ400300.

REFERENCES

[1] Mouritz, A.P., M.K. Bannister, P.J. Falzon and K.H. Leong, Review of applications for advanced three-dimensional fibre textile composites. *Composites Part A: Applied Science and Manufacturing*, 1999. 30(12): p. 1445-1461.

[2] Chou, S., H.-C. Chen and C.-C. Wu, BMI resin composites reinforced with 3D carbon-fibre fabrics. *Composites Science and Technology*, 1992. 43(2): p. 117-128.

[3] Albany International Corp., LEAP Fan Casing. 17th July 2015. Available from: http://www.albany.com/business/aec/en-us/aerospace/Pages/LEAP-Fan-Casing.aspx.

[4] Cox, B.N., M.S. Dadkhah, W.L. Morris and J.G. Flintoff, Failure mechanisms of 3D woven composites in tension, compression, and bending. *Acta Metallurgica et Materialia*, 1994. 42(12): p. 3967-3984.

[5] Cox, B. and M. Dadkhah, The macroscopic elasticity of 3D woven composites. *Journal of Composite Materials*, 1995. 29(6): p. 785-819.

[6] Cox, B.N., M.S. Dadkhah and W.L. Morris, On the tensile failure of 3D woven composites. *Composites Part A: Applied Science and Manufacturing*, 1996. 27(6): p. 447-458.

[7] Tan, P., L. Tong, G.P. Steven and T. Ishikawa, Behavior of 3D orthogonal woven CFRP composites. Part I. Experimental investigation. *Composites Part A: Applied Science and Manufacturing*, 2000. 31(3): p. 259-271.

[8] Lomov, S., M. Karahan, A. Bogdanovich and I. Verpoest, Monitoring of acoustic emission damage during tensile loading of 3D woven carbon/epoxy composites. *Textile Research Journal*, 2014. 84(13): p. 1373-1384.

[9] Kuo, W.-S. and T.-H. Ko, Compressive damage in 3-axis orthogonal fabric composites. *Composites Part A: Applied Science and Manufacturing*, 2000. 31(10): p. 1091-1105.

[10] Kuo, W.-S., T.-H. Ko and C.-P. Chen, Effect of weaving processes on compressive behavior of 3D woven composites. *Composites Part A: Applied Science and Manufacturing*, 2007. 38(2): p. 555-565.

[11] Warren, K.C., R.A. Lopez-Anido and J. Goering, Experimental investigation of three-dimensional woven composites. *Composites Part A: Applied Science and Manufacturing*, 2015. 73: p. 242-259.

[12] Dai, S., P.R. Cunningham, S. Marshall and C. Silva, Influence of fibre architecture on the tensile, compressive and flexural behaviour of 3D woven composites. *Composites Part A: Applied Science and Manufacturing*, 2015. 69: p. 195-207.

[13] Nehme, S., A. Hallal, F. Fardoun, R. Younes, B. Hagege, Z. Aboura, M. Benzeggagh and F.H. Chehade, Numerical/analytical methods to evaluate the mechanical behavior of interlock composites. *Journal of Composite Materials*, 2011. 45(16): p. 1699-1716.

[14] Lu, Z., Y. Zhou, Z. Yang and Q. Liu, Multi-scale finite element analysis of 2.5D woven fabric composites under on-axis and off-axis tension. *Computational Materials Science*, 2013. 79: p. 485-494.
[15] Hallal, A., R. Younes, F. Fardoun and S. Nehme, Improved analytical model to predict the effective elastic properties of 2.5D interlock woven fabrics composite. *Composite Structures*, 2012. 94(10): p. 3009-3028.
[16] ASTM International, ASTM D3039 / D3039M-08, Standard Test Method for Tensile Properties of Polymer Matrix Composite Materials, 2008: West Conshohocken, PA.
[17] Fernie, R., *Loading Rate Effects on the Energy Absorption of Lightweight Tubular Crash Structures*, PhD thesis, University of Nottingham, 2002.
[18] Brown, K.A., R. Brooks, and N.A. Warrior, The static and high strain rate behaviour of a commingled E-glass/polypropylene woven fabric composite. *Composites Science and Technology*, 2010. 70(2): p. 272-283.
[19] ASTM International, ASTM D3518 / D3518M-08, Standard Test Method for In-Plane Shear Response of Polymer Matrix Composite Materials by Tensile Test of a ±45° Laminate, 2008: West Conshohocken, PA.
[20] ASTM International, ASTM D7078 / D7078M-12, Standard test method for shear properties of composite materials by v-notched rail shear method. 2012: West Conshohocken, PA.